Measurement of Quantum Noise in a Carbon Nanotube Quantum Dot in the Kondo Regime

J. Basset,[1] A. Yu. Kasumov,[1] C. P. Moca,[2,3] G. Zaránd,[2,4] P. Simon,[1] H. Bouchiat,[1] and R. Deblock[1]

[1]*Laboratoire de Physique des Solides, Université Paris-Sud, CNRS, UMR 8502, F-91405 Orsay Cedex, France*
[2]*BME-MTA Exotic Quantum Phase Group, Institute of Physics, Budapest University of Technology and Economics, H-1521 Budapest, Hungary*
[3]*Department of Physics, University of Oradea, Oradea, 410087, Romania*
[4]*Freie Universität Berlin, Fachbereich Physik, Arnimallee 14, D-14195 Berlin, Germany*

(Received 6 October 2011; published 24 January 2012)

The current emission noise of a carbon nanotube quantum dot in the Kondo regime is measured at frequencies ν of the order or higher than the frequency associated with the Kondo effect $k_B T_K/h$, with T_K the Kondo temperature. The carbon nanotube is coupled via an on-chip resonant circuit to a quantum noise detector, a superconductor-insulator-superconductor junction. We find for $h\nu \approx k_B T_K$ a Kondo effect related singularity at a voltage bias $eV \approx h\nu$, and a strong reduction of this singularity for $h\nu \approx 3k_B T_K$, in good agreement with theory. Our experiment constitutes a new original tool for the investigation of the nonequilibrium dynamics of many-body phenomena in nanoscale devices.

DOI: 10.1103/PhysRevLett.108.046802 PACS numbers: 73.23.−b, 05.40.Ca, 72.15.Qm, 73.63.Fg

How does a correlated quantum system react when probed at frequencies comparable to its intrinsic energy scales? Thanks to progress in on-chip detection of high frequency electronic properties, exploring the nonequilibrium fast dynamics of correlated nanosystems is now accessible though delicate. In this respect, the Kondo effect in quantum dots is a model many-body system, where the spin of the dot is screened by the contacts' conduction electrons below the Kondo temperature T_K [1–3]. The Kondo effect can then be probed at a single spin level and in out-of-equilibrium situations. It leads to a strong increase of the conductance of the quantum dot at zero bias due to the opening of a spin degenerate conducting channel, the transmission of which can reach unity. This effect has been extensively studied by transport and noise experiments in the low frequency limit [4–11]. However, the noise in the high frequency limit has not been explored experimentally despite the fact that it allows us to probe the system at frequencies of the order of or smaller than $k_B T_K/h$ characteristic of the Kondo effect [12]. In this Letter we present the first high frequency noise measurements of a carbon nanotube quantum dot in the Kondo regime. We find for $h\nu \approx k_B T_K$ a Kondo effect related singularity at a voltage bias $eV \approx h\nu$, and a strong reduction of it for $h\nu \approx 3k_B T_K$. These results are compared to recent theoretical predictions.

The high frequency current fluctuations are measured by coupling the carbon nanotube (CNT) to a quantum noise detector, a superconductor-insulator-superconductor (SIS) junction, via a superconducting resonant circuit [see Fig. 1(a)]. This allows us to probe the emission noise of the CNT at the resonance frequencies of the coupling circuit (29.5 and 78 GHz) by measuring the photoassisted tunneling current through the detector [13]. The probed sample consists of two coupled coplanar transmission lines. One line is connected to the ground plane via a carbon nanotube and the other via a superconducting tunnel junction of size 240×150 nm^2 (Fig. 1). Each transmission line consists of two sections of same length l but different widths, thus different characteristic impedances $Z_1 \approx 110\Omega$ and $Z_2 \approx 25\Omega$ [Fig. 1(a)]. Because of the impedance mismatch, the transmission line acts as a quarter wavelength resonator, with resonances at frequencies $\nu_n = n\nu/4l = n\nu_1$, with ν the propagation velocity and n an odd integer [13]. The two transmission lines are close to one another to provide a good coupling at resonance and are terminated by on-chip Pd resistors. The junction has a SQUID geometry to tune its critical current with a magnetic flux. The carbon nanotube (CNT) is first grown by chemical vapor deposition on an oxidized undoped silicon wafer [14]. An individual CNT is located relative to predefined markers and contacted to palladium leads using electron-beam lithography. The junction and the resonator are then fabricated in aluminum (superconducting gap $\Delta = 182$ μeV). A nearby side gate allows us to change the electrostatic state of the nanotube. The system is thermally anchored to the cold finger of a dilution refrigerator of base temperature 20 mK and measured through low-pass filtered lines with a standard low frequency lock-in amplifier technique.

To characterize the CNT-quantum dot, we first measure its differential conductance dI/dV_S as a function of dc bias voltage V_S and gate voltage V_G [Fig. 1(c)]. For a gate voltage between 3.05 and 3.2 V the CNT's conductance at zero bias strongly increases, a signature of the Kondo effect. The half width at half maximum (HWHM) of the Kondo ridge yields the Kondo temperature $T_K = 1.4$ K in the center of the ridge [1]. This value is also consistent with the temperature dependence of the zero bias conductance. The Kondo temperature is related to the charging energy U

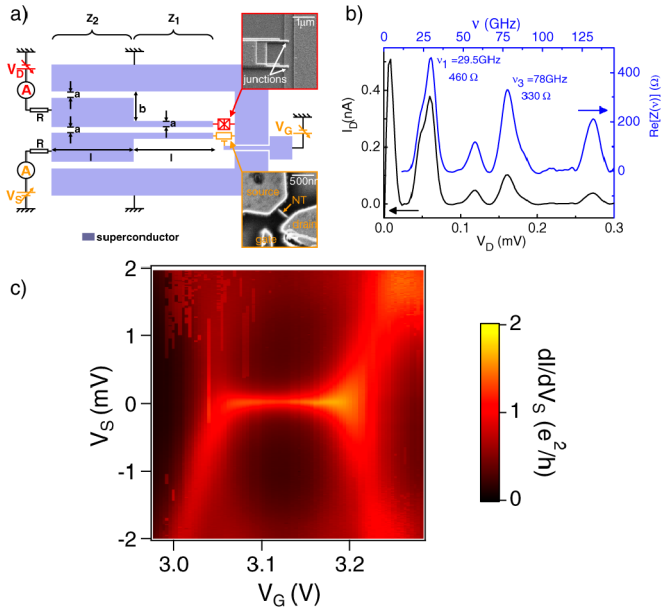

FIG. 1 (color online). (a) Sketch of the sample: a carbon nanotube (bottom electron microscope picture) is coupled to a superconductor-insulator-superconductor (SIS) junction (top electron microscope picture), used as a quantum detector, by a superconducting resonant circuit. This circuit is constituted by two transmission lines, placed close to one another, made of aluminum and terminated by on-chip Pd resistors. The SIS junction is fabricated by shadow angle evaporation. The carbon nanotube is CVD grown, connected with palladium contacts and side gated. (b) Lower curve: $I(V)$ of the detector in the subgap region. Upper curve: the real part of the impedance seen by the detector exhibits several resonances. (c) Differential conductance dI/dV_S of the carbon nanotube as a function of voltage bias V_S and gate voltage V_G. It exhibits a Kondo ridge for gate voltage between 3.05 and 3.20 V with an increase of conductance at zero bias.

of the CNT-quantum dot, the coupling Γ to the electrodes, and the position ϵ of the energy level measured from the center of the Kondo ridge, according to Bethe ansatz [15,16]:

$$T_K = \sqrt{U\Gamma/2}\exp\left[-\frac{\pi}{8U\Gamma}|4\epsilon^2 - U^2|\right]. \quad (1)$$

From $U = 2.5$ meV, deduced from the size of the Coulomb diamond, and $T_K = 1.4$ K, we obtain $\Gamma = 0.51$ meV. The asymmetry $A = (\Gamma_L - \Gamma_R)/(\Gamma_L + \Gamma_R) = 0.67$ of the contacts is deduced from the zero bias conductance.

To characterize the superconducting resonant circuit which couples the detector junction to the CNT, we measure the subgap $I(V)$ characteristic of the junction which depends on the impedance of its electromagnetic environment [17]. In the case of a superconducting transmission line resonator [13,18], resonances appear in the subgap region $V_D < 2\Delta/e$ due to the excitation of the resonator modes by the ac Josephson effect [19]. These resonances are related to the real part of the impedance $Z(\nu)$ seen by the junction

$$I(V_D) = \mathrm{Re}[Z(2eV_D/h)]I_C^2/2V_D, \quad (2)$$

with $I_C = \pi\Delta/(2eR_N)$ the critical current [19], $R_N = 28.6k\Omega$ the normal state resistance of the junction, and Δ the superconducting gap of the electrodes. Equation (2) accounts for the effect of the electromagnetic environment on the tunneling of Cooper pairs through the Josephson junction [17]. Figure 1(b) shows the $I(V)$ of the junction in the subgap region for I_C maximized with magnetic flux. The subgap resonances thus yield via Eq. (2) $\mathrm{Re}[Z(\nu)]$ [Fig. 1(b)] which is peaked at frequencies $\nu_1 = 29.5$ and $\nu_3 = 78$ GHz. Using the height and width of the resonance peaks of $\mathrm{Re}[Z(\nu)]$, we infer the coupling between the junction and the CNT [13]. We then translate a photo-assisted tunneling (PAT) quasiparticles current measurement into a current emission noise measurement for the frequencies ν_1 and ν_3. The ratio r_n between the measured PAT current through the detector and the current emission noise of the CNT at a given resonance frequency is estimated as follows. r_n is given at the resonant frequency ν_n by $e^2|Z_t(\nu_n)|^2\delta\nu_n/(h\nu_n)^2 I_{QP,0}(V_D + \frac{h\nu_n}{e})$ with Z_t the transimpedance of the coupling circuit, defined as the ratio between the voltage fluctuations across the detector and the current fluctuations through the source, $\delta\nu_n$ the width of the resonance peak, and $I_{QP,0}(V_D)$ the I-V characteristic of the detector [13]. This value has been calibrated in a previous experiment with the same design as the one used in the present work [13]. r_n is then calculated using the ratio of the calibrated sample corrected according to the square area under the corresponding peak of $\mathrm{Re}[Z(\nu)]$ [Fig. 1(b)], the value of ν_n, the superconducting gap and the tunnel resistance of the detector junction.

To measure the quantum noise of the CNT, we modulate its bias voltage V_S and monitor the modulated part of the PAT current through the detector for a given detector bias voltage V_D. V_D selects the frequency range of the measurement [13]. We have thus access to the derivative of the PAT current versus CNT bias voltage dI_{PAT}/dV_S at a given frequency. Using the previously estimated coupling coefficient, we translate this quantity into the derivative of the current noise S_I at one of the resonance frequencies versus V_S, dS_I/dV_S. This quantity is plotted in the center of the Kondo ridge, i.e., $\epsilon = 0$ at two frequencies [Figs. 2(a) and 2(b)]. For each frequency, the data exhibit a region close to $V_S = 0$ where $dS_I/dV_S = 0$. This corresponds to $|eV_S| < h\nu$, where the system does not have enough energy to emit noise at a frequency ν. The observation of this zero noise region is a strong evidence that we are indeed only measuring the emission noise of the CNT. For $|eV_S| > h\nu$ the system emits noise at ν. For the first resonance frequency $\nu_1 = 29.5$ GHz, with $h\nu_1 \approx k_B T_K$, the measured derivative of the noise shows a singularity for bias voltages close to the measured frequency. At higher bias voltages

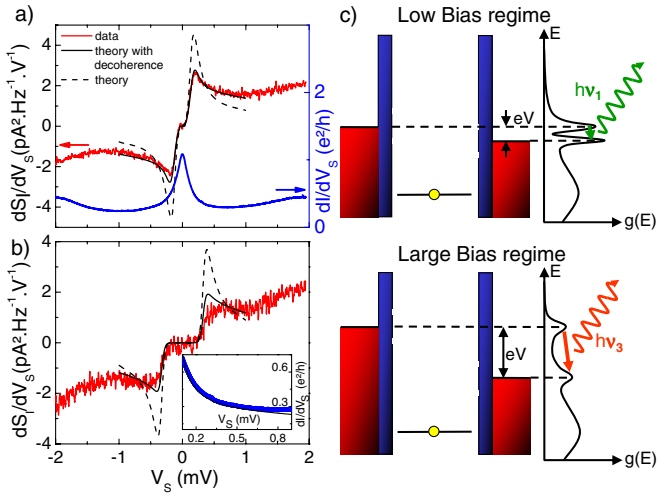

FIG. 2 (color online). (a) Derivative of the current noise and differential conductance of the CNT versus V_S in the center of the Kondo ridge. Left axis: measured dS_I/dV_S (in red) at 29.5 GHz as a function of bias voltage V_S. The black solid line corresponds to the calculated dS_I/dV_S with a fitted decoherence rate incorporating both intrinsic and extrinsic decoherence (see text), while the dashed line is the theoretical prediction with the intrinsic decoherence rate. Right axis: Differential conductance dI/dV_S of the CNT in units of e^2/h. (b) Same data at 78 GHz. Inset: measured conductance, symmetrized with respect to the bias voltage, in units of e^2/h. The black solid line corresponds to the FRG calculation of the conductance with the same fitted decoherence rate as the one used for the noise measurements. (c) Schematic picture of a quantum dot in the out-of-equilibrium Kondo regime together with the density of states for two distinct bias voltages. When the quantum dot is voltage biased, the Kondo resonance splits in two with a splitting given by the applied bias voltage. This leads to an increase of the emission at frequency $eV_S = h\nu$. The amplitude of the resonance peaks, and thus the emission noise at $eV_S = h\nu$, can be reduced by decoherence effects induced by the applied bias voltage.

dS_I/dV_S is much smoother. For $h\nu_3 \approx 2.7 k_B T_K$ the previous singularity is nearly absent and dS_I/dV_S versus V_S is practically flat.

The high frequency noise of quantum dots in the Kondo regime has been studied theoretically at equilibrium using the numerical renormalization group (NRG) technique [20]. Nonequilibrium results for the finite-frequency noise are theoretically much more demanding. They were obtained only for peculiar values of parameters (strongly anisotropic exchange couplings) of the Kondo problem using bosonization methods [21], and by using nonequilibrium real time renormalization group approaches [22,23]. The latter approaches assume $h\nu, eV_S \gg k_B T_K^{\mathrm{RG}}$, with T_K^{RG} the Kondo temperature defined from the renormalization group. Importantly, T_K^{RG} differs from T_K (defined experimentally as the HWHM of the differential conductance) by a numerical factor, which has to be determined (see below). Here we employ the real time functional renormalization group (FRG) approach developed in Ref. [23] to compute the nonequilibrium frequency-dependent noise and compare it to the experimental results. We perform the nonequilibrium calculations using the Kondo Hamiltonian, given by

$$H_K = \frac{1}{2} \sum_{\alpha,\beta=L,R} \sum_{\sigma,\sigma'} j_{\alpha\beta} \psi^\dagger_{\alpha\sigma} \mathbf{S} \cdot \boldsymbol{\sigma}_{\sigma\sigma'} \psi_{\beta\sigma'}. \qquad (3)$$

Here the $j_{\alpha\beta}$ denote the Kondo couplings, α, β are indices for the left (L) and right (R) leads, $\boldsymbol{\sigma}$ stands for the three Pauli matrices, and the operator $\psi_{\alpha\sigma}$ destroys an electron of spin σ in lead $\alpha \in \{L, R\}$. We parametrize the dimensionless exchange couplings $j_{\alpha\beta}$ as $j_{\alpha\beta} = j\upsilon_\alpha\upsilon_\beta$, with the factors $\{\upsilon_L, \upsilon_R\} = \{\cos(\phi/2), \sin(\phi/2)\}$ accounting for the asymmetry of the quantum dot, $\cos(\phi) = A$, and ϕ related to the $T = 0$ conductance as $G(T = 0) = (2e^2/h)\sin^2(\phi)$.

The Kondo Hamiltonian assumes that charge fluctuations in the CNT-quantum dot are frozen. Therefore, the theoretical results based on (3) can and shall be compared with experimental ones only for bias voltages $V_S \ll U/e$. As a first step, to determine the ratio T_K^{RG}/T_K, we computed the equilibrium conductance by using NRG [24] and compared it to experimental data in the center of the Kondo ridge ($\epsilon = 0$). This enabled us to establish $T_K \approx 3.7 T_K^{\mathrm{RG}}$ (see the Supplemental Material [25]). Therefore, the condition $h\nu \gg k_B T_K^{\mathrm{RG}}$ for our FRG approach to apply is certainly met for the frequency ν_3, and still reasonably satisfied for ν_1.

Within the Kondo model, we can express the Fourier transform of the emission noise S_I as

$$S_I(V_S, \nu) = \frac{e^2}{h} k_B T_K^{\mathrm{RG}} s\left(\frac{eV_S}{k_B T_K^{\mathrm{RG}}}, \frac{h\nu}{k_B T_K^{\mathrm{RG}}}, \frac{T}{T_K^{\mathrm{RG}}}, A\right), \qquad (4)$$

where s is a dimensionless function, which we calculate by solving numerically the FRG equation (see [25]). Since the measurement temperature satisfies $T \ll T_K$, we have taken $T = 0$ in the calculations and checked that a finite but small temperature does not affect our results. Note that no fitting parameter has been included at this level, since the asymmetry parameter A and $T_K^{\mathrm{RG}} \approx 0.38$ K were extracted from the experimental data. The dashed lines in Figs. 2(a) and 2(b) show the calculated dS_I/dV_S curves for frequencies $\nu_1 = 29.5$ GHz and $\nu_3 = 78$ GHz, respectively. The computed curves are only shown in the bias range $|V_S| < 1$ mV, where the Kondo Hamiltonian in Eq. (3) is appropriate to describe the physics of the CNT-quantum dot. For both frequencies, the theoretical curves exhibit sharp singularities at $eV_S = h\nu$, much more pronounced than the experimental ones. This especially holds for the resonance frequency, $\nu_3 = 78$ GHz, where the resonance is almost completely absent experimentally. The singularity at the threshold $eV_S \approx h\nu$ is related to the existence of two Kondo resonances associated with the Fermi levels of the two contacts. Inelastic transitions

between them lead to an increase of dS_I/dV_S for frequencies corresponding to the energy separation, $h\nu \approx eV_S$ [Fig. 2(c)].

To compute the dashed curves in Fig. 2, an intrinsic spin decoherence time τ_S induced by the large bias was included and calculated self-consistently in the FRG approach [26] (see SM). The decoherence of the Kondo effect induced by a large dc voltage bias is a well-known feature which has indeed been measured [27,28], and has been predicted to lead to a strong reduction of the Kondo resonance due to inelastic processes [26,29,30]. Since the singularity in the noise at $h\nu \approx eV_S$ is associated with the transitions between the two Kondo resonances pinned at the Fermi levels of the contacts, this singularity is also affected by decoherence.

However, as shown in Fig. 2, the computed intrinsic decoherence time is insufficient to explain the experimentally observed suppression of the peak in dS_I/dV_S. Therefore, we incorporated a voltage-dependent spin relaxation rate in our calculations, $\tau_S^{-1}(V_S)$, which includes external decoherence. The consistency of this approach can be checked against the experiments: a single choice of $\tau_S^{-1}(V_S)$ must simultaneously reproduce the voltage dependence of the differential conductance through the dot $dI/dV_S(V_S)$, and those of the $\nu_1 = 29.5$ GHz and $\nu_1 = 78$ GHz noise spectra, $dS_I/dV_S(V_S)$. Furthermore, τ_S^{-1} should be suppressed for $V_S < T_K^{\mathrm{RG}}$. We found that a bias-dependent decoherence rate of the form $h/\tau_S \approx \alpha k_B T_K^{\mathrm{RG}} \arctan(\beta eV_S/k_B T_K^{\mathrm{RG}})$ (similar in shape to the calculated intrinsic spin relaxation rates), with $\alpha = 14$ and $\beta = 0.15$ satisfied all criteria above. The continuous lines in Fig. 2 show the dS_I/dV_S curves computed with this form of h/τ_S, and fit fairly well the experimental data for both resonator frequencies. As a final consistency check, we also computed the differential conductance through the dot (taking into account the above form of τ_S^{-1}) and compared it to the measured dI/dV_S curves. A very good agreement is found without any other adjustable parameter in the voltage range $V > 0.1$ mV, where the FRG approach is appropriate [inset of Fig. 2(b)].

From the theoretical fits we infer that the experimentally observed noise spectra and differential conductance can be understood in terms of a decoherence rate, which is about a factor of 2 larger than the theoretically computed intrinsic rate (see [25]). One possibility for this discrepancy is that the experimentally observed decoherence is intrinsic, and FRG—which is a perturbative approach—underestimates the spin relaxation rate in this regime (which is indeed almost out of the range of perturbation theory). Another possibility is that the experimental setup leads to additional decoherence.

The experiment also allows us to draw a complete map of the noise in the region of the Kondo ridge. We define $F(V_S) = [dS_I/dV_S(V_S)]/[edI/dV_S(V_S - h\nu/e)]$, i.e., the ratio of the derivative of the noise to the differential conductance shifted in voltage by an amount corresponding to the measured frequency. For both linear and nonlinear systems with energy independent transmission at low temperature this quantity is equal to the Fano factor [31]. We have plotted $F(V_S)$ for $\nu_1 = 29.5$ GHz [Fig. 3(a)] and $\nu_3 = 78$ GHz [Fig. 3(b)]. For $|eV_S| < h\nu$, where the emission noise is zero, $F(V_S)$ is arbitrarily fixed to zero. For both frequencies the noise is found to be sub-Poissonian, with $F(V_S)$ close to 1 in the poorly conducting regions and a strong decrease of $F(V_S)$ along the conducting regions. This is qualitatively consistent with the reduction of the Fano factor for a conducting channels of transmission close to 1. This result has to be contrasted with backscattering noise measurements in the Kondo regime at low frequency and low bias voltage where the Fano factor was found to be higher than one [10,11].

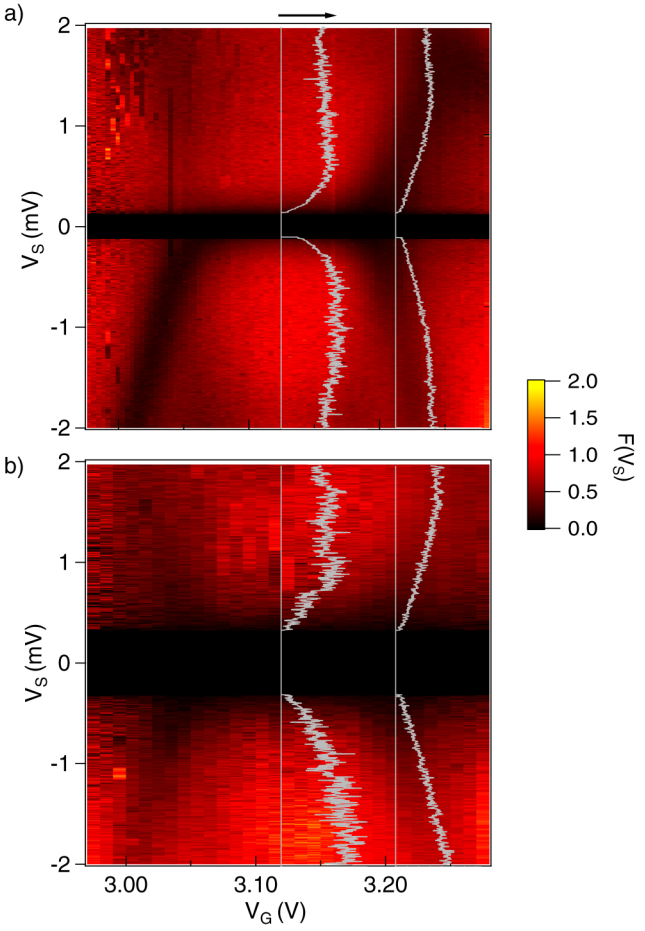

FIG. 3 (color online). $F(V_S) = [dS_I/dV_S]/[edI/dV_S(V_S - h\nu/e)]$ as a function of the bias voltage V_S and the gate voltage V_G at $\nu_1 = 29.5$ GHz (a) and $\nu_3 = 78$ GHz (b). $F(V_S)$ is arbitrarily fixed to zero for $e|V_S| < h\nu$. The gray curves on top of the color plot correspond to the bias voltage dependence of $F(V_S)$ at $V_G = 3.12$ V and $V_G = 3.21$ V. The black arrow indicates a value of the $F(V_S)$ equal to 1. When the conductance is low, $F(V_S)$ is close to 1 while it is reduced in the highly conducting regions.

In conclusion, we have measured the high frequency current fluctuations of a carbon nanotube quantum dot in the Kondo regime by coupling it to a quantum detector via a superconducting resonant circuit. We find that the noise exhibits strong resonances when the voltage bias is of the order of the measurement frequency in good agreement with theory provided that an additional decoherence rate is included which prevents the full formation of the out-of-equilibrium Kondo resonances. Our experiment constitutes a new original tool for the investigation of the nonequilibrium dynamics of many-body phenomena in nanodevices.

We thank M. Aprili, S. Guéron, M. Ferrier, M. Monteverde, and J. Gabelli for fruitful discussions. This work has benefited from financial support of ANR under Contract No. DOCFLUC (ANR-09-BLAN-0199-01) and C'Nano Ile de France (project HYNANO), the EU-NKTH GEOMDISS project, OTKA research Grants No. K73361 and No. CNK80991 and the French-Romanian Grant No. DYMESYS (ANR 2011-IS04-001-01 and Contract No. PN-II-ID-JRP-2011-1).

[1] D. Goldhaber-Gordon *et al.*, Nature (London) **391**, 156 (1998).
[2] S. M. Cronenwett, T. H. Oosterkamp, and L. P. Kouwenhoven, Science **281**, 540 (1998).
[3] J. Nygard, D. H. Cobden, and P. E. Lindelof, Nature (London) **408**, 342 (2000).
[4] Y. Meir and A. Golub, Phys. Rev. Lett. **88**, 116802 (2002).
[5] E. Sela, Y. Oreg, F. von Oppen, and J. Koch, Phys. Rev. Lett. **97**, 086601 (2006).
[6] A. Golub, Phys. Rev. B **73**, 233310 (2006).
[7] A. O. Gogolin and A. Komnik, Phys. Rev. Lett. **97**, 016602 (2006).
[8] C. Mora, X. Leyronas, and N. Regnault, Phys. Rev. Lett. **100**, 036604 (2008).
[9] T. Delattre *et al.*, Nature Phys. **5**, 208 (2009).
[10] O. Zarchin, M. Zaffalon, M. Heiblum, D. Mahalu, and V. Umansky, Phys. Rev. B **77**, 241303(R) (2008).
[11] Y. Yamauchi *et al.*, Phys. Rev. Lett. **106**, 176601 (2011).
[12] P. Nordlander, M. Pustilnik, Y. Meir, N. S. Wingreen, and D. C. Langreth, Phys. Rev. Lett. **83**, 808 (1999).
[13] J. Basset, H. Bouchiat, and R. Deblock, Phys. Rev. Lett. **105**, 166801 (2010).
[14] Yu. A. Kasumov *et al.*, Appl. Phys. A **88**, 687 (2007).
[15] A. M. Tsvelick and P. B. Wiegmann, Adv. Phys. **32**, 453 (1983).
[16] N. E. Bickers, Rev. Mod. Phys. **59**, 845 (1987).
[17] G. Ingold and Y. V. Nazarov, *Single-Charge Tunneling*, edited by H. Grabert and M. H. Devoret (Plenum, New York, 1992).
[18] T. Holst, D. Esteve, C. Urbina, and M. H. Devoret, Phys. Rev. Lett. **73**, 3455 (1994).
[19] A. Barone and G. Paterno, *Physics and Applications of the Josephson Effect* (Wiley-Interscience, New York, 1982).
[20] M. Sindel, W. Hofstetter, J. von Delft, and M. Kindermann, Phys. Rev. Lett. **94**, 196602 (2005).
[21] A. Schiller and S. Hershfield, Phys. Rev. B **58**, 14 978 (1998).
[22] T. Korb, F. Reininghaus, H. Schoeller, and J. König, Phys. Rev. B **76**, 165316 (2007).
[23] C. P. Moca, P. Simon, C. H. Chung, and G. Zarand, Phys. Rev. B **83**, 201303(R) (2011).
[24] We used the open access Budapest DM-NRG code, http://neumann.phy.bme.hu/~dmnrg/.
[25] See Supplemental Material at http://link.aps.org/supplemental/10.1103/PhysRevLett.108.046802 for theoretical details.
[26] J. Paaske, A. Rosch, J. Kroha, and P. Wölfle, Phys. Rev. B **70**, 155301 (2004).
[27] S. De Franceschi *et al.*, Phys. Rev. Lett. **89**, 156801 (2002).
[28] R. Leturcq *et al.*, Phys. Rev. Lett. **95**, 126603 (2005).
[29] R. C. Monreal and F. Flores, Phys. Rev. B **72**, 195105 (2005).
[30] R. Van Roermund, S.-y. Shiau, and M. Lavagna, Phys. Rev. B **81**, 165115 (2010).
[31] Y. M. Blanter and M. Büttiker, Phys. Rep. **336**, 1 (2000).